J Porous Mater (2012) 19:181–188
DOI 10.1007/s10934-011-9458-9

Tailoring the pore structure of PCL scaffolds for tissue engineering prepared via gas foaming of multi-phase blends

A. Salerno · E. Di Maio · S. Iannace · P. A. Netti

Published online: 8 February 2011

Abstract The aim of this study was the design of poly(ε-caprolactone) (PCL) scaffolds characterized by well controlled pore structures obtained by gas foaming of multi-phase blends of PCL and thermoplastic gelatin (TG). Co-continuous blends made of PCL and TG were prepared by melt mixing and, subsequently gas foamed in an autoclave to induce the formation of the porous network. A mixture of N_2 and CO_2 was used as blowing agent and the foaming process performed at temperature higher than PCL melting, in the range 70–110 °C. The foams were finally soaked in water at 37 °C to selectively extract the TG and achieve the final pore structure. The results of this study demonstrated that the proposed approach allowed to tailor the micro-structural properties of PCL scaffolds for tissue engineering.

Keywords Gas foaming · PCL · Pore structure · Scaffold · Tissue engineering

A. Salerno (✉) · P. A. Netti
Interdisciplinary Research Centre on Biomaterials (CRIB), P.le Tecchio 80, 80125 Naples, Italy
e-mail: asalerno@unina.it

A. Salerno · P. A. Netti
Italian Institute of Technology (IIT), P.le Tecchio 80, 80125 Naples, Italy

A. Salerno · S. Iannace
Institute of Composite and Biomedical Materials, National Research Council (IMCB-CNR), P.le Tecchio 80, 80125 Naples, Italy

E. Di Maio · P. A. Netti
Department of Materials and Production Engineering, University of Naples Federico II, P.le Tecchio 80, 80125 Naples, Italy

1 Introduction

Current approaches in tissue engineering (TE) for the repair/regeneration of damaged and/or malfunctioned biological tissues involve three main components, namely cells, scaffolds and bioactive moieties [1, 2]. In this approach, the scaffold serve as 3D substrate for cells adhesion, proliferation and biosynthesis, ultimately defining the final internal properties and external shape of new-engineered tissues [1, 2]. TE scaffolds are porous biocompatible and biodegradable materials characterized by well controlled pore structure, mechanical function and biodegradation rate [3–6]. The pore network of the scaffold must promote and guide biological processes involved in new-tissue genesis, along with fluid transport in three dimensions [3–6]. The scaffold must also ensure a physical structure that progressive degrades, with degradation and resorption rates matching the rate of new-tissue production by the cells [4, 6]. All of these key micro-structural scaffold design properties are strongly dependent on scaffold materials and pore structure.

Porosity is necessary for new-tissue formation because it allows for the migration and proliferation of cells in three dimensions, as well as tissue vascularization [1, 4–7]. In addition, a porous surface improves mechanical interlocking between the implant and the surrounding tissue, providing greater mechanical stability at this critical interface [7]. Several studies investigated the effect of scaffold porosity and pore size on the in-growth and differentiation of specific cell type [4, 5, 7–14]. For instance, Freed et al. reported that an ideal scaffold should possess an overall porosity of 90% to allow for the adequate fluid diffusion and cell infiltration in vitro [11]. Nevertheless, Hollister et al. have indicated that a porosity degree of 50–60% may allow for the optimal design of the mechanical function of poly(ε-caprolactone) (PCL) scaffolds for hard tissue repair/regeneration [5].

Regarding scaffold pore size, in vitro and in vivo experimental tests demonstrated that, in the case of neo-vascularization, optimal pore size is 35 μm [12], while 150–200 μm pore size is suitable for fibroblasts in-growth [13], 20–80 μm hepatocytes in-growth [15] and 100–500 μm for regeneration of bone [4, 5, 14]. Although these results are dependent on the specific TE scaffold material/application, they clearly demonstrated that the success of any TE scaffold approach reside on the development of process technologies able to imprint well controlled pore structures within biocompatible and biodegradable materials.

PCL is one of the most investigated Food and Drug Administration (FDA)-approved biodegradable polymers for TE applications [1, 4–6, 10, 13]. Indeed, PCL may be easily processed in order to prepare scaffolds with hierarchical pore structures within arbitrary and complex anatomical shapes [5, 10]. Porous PCL scaffolds have been therefore used for several TE applications, including the in vitro culture of stem cells, chondrocytes, osteoblasts, and fibroblasts as well as the in vivo bone regeneration [5, 10, 13].

Among the process technologies that have been developed and successful implemented for the design of TE scaffolds, gas foaming (GF) has recently attracted much attention. Indeed, by this technique it has been possible the design of 3D porous scaffolds with well controlled porosity and pore size distribution spanning from several biocompatible and biodegradable materials [15–17]. GF alone may not be suitable for achieving high degrees of pore interconnectivity, and it is typically combined with other techniques, such reverse templating [10, 18]. For instance, we recently reported the possibility of preparing PCL scaffolds with mono-modal or bi-modal pore size distributions by GF multi-phase blends of PCL and thermoplastic gelatin (TG) [10]. Along with this research line, in this study we prepared a PCL/TG co-continuous blend and investigated the design of PCL scaffolds with well controlled pore structures and mechanical responses via the GF process. To this aim, we investigated the effect of foaming temperature on the morphology of the PCL/TG foams as well as the morphology, porosity, pore size distribution and mechanical properties of PCL scaffolds after the selective TG removal. Finally, in vitro hMSCs culture has been performed to assess the biocompatibility of the as obtained PCL scaffolds.

2 Experimental section

2.1 Materials

PCL (M_W = 65 kDa, T_m = 59–64 °C, T_g = −60 °C and ρ = 1.145 g/cm^3) and gelatin powder (type B, M_W = 40–50 kDa) were purchased from Sigma–Aldrich (Italy). Glycerol anhydrous was purchased by Fluka (Italy) and used as plasticizer for the thermoplasticization of gelatin. N_2/CO_2 (4/1 vol% ratio) mixture was purchased by Air liquide (Italy) as used as blowing agent for the GF process.

2.2 Scaffold preparation

The TG and PCL/TG co-continuous blend were prepared as described previously [10, 19]. Briefly, TG was prepared first by mixing gelatin and glycerol (4/1 wt ratio) in an internal mixer equipped with a mixing device (Rheomix® 600 Haake, Germany) and a controller unit (Haake Rheocord® 9000) at 60 °C, 60 rpm for 6 min. The TG was subsequently blended with PCL (2/3 wt% ratio) at 60 °C, 80 rpm for 6 min. The co-continuous PCL/TG blend was then compressed at 70 °C and 30 bar into 3 mm-thick plates by a P 300 P hot press (Collin, Germany).

For GF experiments, disc-shaped samples (d = 10 mm and h = 3 mm) were solubilized with the blowing agent in an autoclave (HiP, US) at 70 °C, 180 bar for 4 h. After solubilization, the autoclave was heated to the foaming temperature, selected in the 70–110 °C range and, the pressure quenched to the ambient at a pressure drop rate of 700 bar/s. [10, 12]. The autoclave was then rapidly cooled to the ambient and the samples extracted for the leaching of TG, conducted by soaking the foamed blends in H_2O at 38 °C for 1 week. Samples were finally dried under vacuum at room temperature for 1 day.

2.3 Scaffold characterization

The morphology of the PCL/TG foamed blend before and after TG leaching was analyzed by scanning electron microscopy (SEM) and image analysis. The samples were cross-sectioned by a razor blade, gold sputtered and analyzed by SEM (LEICA S440) working at 20 kV. Image analysis was used in order to assess the pore size and distribution of the samples starting from the SEM micrographs. In particular, the SEM micrographs were converted to 8-bit digital images and analyzed by Image J® software in order to evaluate the pore size distributions and the mean pore size (ASTM D3576). At least 100 pores for each scaffold type were used for the analysis.

The overall porosity of the PCL scaffolds resulting from the TG leaching was evaluated by using the following equation [10]:

$$\% \text{ porosity} = [1 - (\rho_S/\rho_{PCL})] \times 100$$

where ρ_S is the apparent density of the scaffold calculated from mass and volume measurements and ρ_{PCL} the density of neat PCL at atmospheric conditions. The mass was measured by using a high accuracy balance (10^{-3} g, AB104-S, Mettler Toledo, Italy), while the volume determined by

geometrical calculation. The overall porosity data represents the mean value of five different measurements.

The percentage of TG leached out from the foamed PCL/TG blend was evaluated by gravimetric measurements. The samples were weighted before and after leaching to assess the weight loss and, the results compared to the nominal TG concentration. Five measurements were performed for each scaffold type and the results compared to those achieved for neat PCL/TG blend.

Infrared spectroscopic measurements were carried out by using a Necsus-Nicolet spectrophotometer with a detection resolution of 0.1 wt%, in order to analyze the effect of the GF/PE process on the chemical structure of the scaffolds and to qualitatively assess the presence of gelatin residues within the scaffolds after the TG extraction. The scaffolds were compression molded at 90 °C and 100 bar in order to prepared 10 μm thick films and, analyzed collecting 32 scans for each sample at a resolution of 1 cm^{-1}. The FTIR analysis was additionally performed of neat PCL and TG films for comparison.

The static compression properties of the scaffolds were determined using an Instron mechanical testing system (4204, Instron, Italy), working at a cross head speed of 1 mm/min and with a 1 kN loading cell. A small preload was applied to each sample to ensure that, prior to testing, the entire scaffold surface was in contact with the compression plates. Five disc-shaped scaffolds ($d = 10$ mm and $h = 4$ mm) were tested for each scaffold type and the elastic compression modulus E was determined as the slope of the initial linear portion of the stress versus strain curve.

The biocompatibility of the PCL scaffolds was assessed in vitro by using human bone marrow derived mesenchymal stem cells (hMSCs, Clonetics, Italy), following the protocol described in [10]. Briefly, γ-sterilized disc-shaped scaffolds ($d = 10$ mm and $h = 3$ mm) were statically seeded with $1*10^5$ MSCs, resuspended in 50 μL of medium. The scaffolds were then incubated for 2 h at 37 °C and 5% CO_2, to allow cell attachment and, subsequently, cell culture medium was added to each well to bring the total well volume to 1.5 mL. The cell/scaffold constructs were maintained in culture for 1 week. To assess hMSCs adhesion and spatial distribution, the cell/scaffold constructs were cryostat sectioned, transversal to the seeding surface, to obtain 50 μm thick slices. The cell/scaffold sections were then stained by using haematoxylin–eosin (H–E) solutions following standard procedure and, analyzed by an optical microscope (CK40, Olympus, Italy).

3 Results and discussion

In the past twenty years, the increasing demand of porous scaffolds with well controlled micro-structural properties has driven the scientific efforts of the TE community towards the development of novel approaches capable to imprint well controlled porosity patterns within biocompatible and biodegradable materials. In this study we investigated the design of porous PCL scaffolds via GF of multi-phase PCL/TG blend and, we evaluated the effect of the foaming temperature on the PCL scaffold porosity and pore size distribution, mechanical properties and biocompatibility.

GF with physical blowing agents, such as CO_2, N_2 and theirs mixtures, have been widely used for the design of porous TE scaffolds, [10, 15–18]. Indeed, this technique allows the control of scaffold pore structure by the appropriate selection of the processing parameters, mainly blowing agent type and foaming temperature [15–17]. Furthermore, when combined with reverse templating techniques, GF allowed the design of porous scaffolds with enhanced pore interconnectivity and highly complex architectures [10, 18].

As shown in Fig. 1, the PCL/TG foams were characterized by multi-phase morphologies and bi-modal pore structures. In particular, for all the foaming temperature range investigated, we observed the presence of a porous network within the PCL phase with big coalesced pores. Concomitantly, the TG phase evidenced homogeneous and uniformly distributed pores, characterized by smaller size if compared to the pores of the PCL phase (low and high magnifications reported in Fig. 1). The heterogeneous pore structure of PCL/TG foamed blend may be ascribed to several factors, mainly the heterogeneous micro-structure of PCL/TG blend and the foaming properties of pure polymers. Indeed, the initial blend composition, in the co-continuous range for the system under investigation, may ensure the presence of two immiscible and interpenetrated PCL and TG networks, acting in a synergistic fashion during blowing agent solubilization and foaming. In particular, the selection of foaming temperatures in the 70–110 °C range, higher than PCL melting temperature, induced the foaming and subsequent collapse of PCL, because the polymer is unable to crystallize and stabilize the pore structure. However, the presence of the interpenetrated TG network, that is physically stable in this temperature range [19], make the foams stable and allowed the PCL to collapse at the interface with TG (Fig. 1). Furthermore, as usually observed for other thermoplastic materials [16, 19], the increase of the foaming temperature from 70 to 110 °C resulted in the increases of the foaming, even if the foamed blend showed bi-modal morphologies. Therefore, at higher foaming temperatures we observed foams characterized by larger PCL and TG pores.

These considerations were supported by the results of the mean pore size of PCL and TG phases of the multi-phase foams reported in Fig. 2. The two polymers were characterized by one order of magnitude different pore size while, the pore size increased with the increase of the

foaming temperature for both PCL and TG. In particular, for the PCL phase we observed a mean pore size equal to 190 ± 81 μm at 70 °C, that increased to 620 ± 386 μm at 110 °C. Concomitantly, the mean pore size of TG phase increased from 14.7 ± 12.3 μm to 51.3 ± 37.4 μm when the foaming temperature increased from 70 to 110 °C, respectively.

The final PCL scaffolds were obtained after the selective extraction of TG from the foamed PCL/TG blend. Although TG residues within the PCL scaffolds could not expected to be harmful for cells and tissues, one of the prerequisite of the proposed PCL scaffold design approach is the complete extraction of the templating agent. The results of the percentage of TG extracted from the foams were reported in Fig. 3, together with the percentage of TG extracted from neat PCL/TG blend. All the samples showed an efficiency of TG extracted close to 100%, indicating that the additional foaming process did not affect the co-continuity of the two polymeric phases. Nevertheless, taking into account that these values were evaluated by dividing the weight loss to the nominal TG concentration into the initial blend, in some cases we observed a TG extraction efficiency higher than 100%.

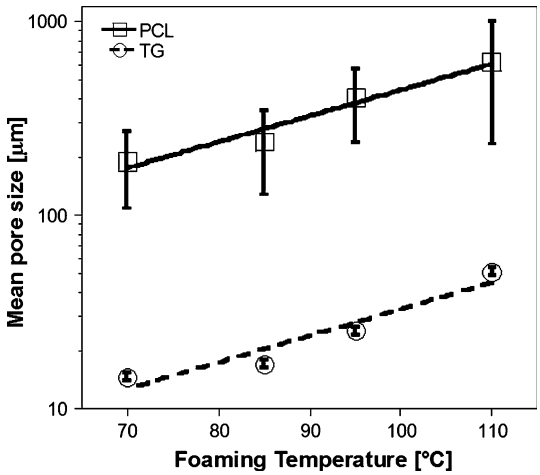

Fig. 2 Effect of foaming temperature on the mean pore size of PCL and TG phases

The FTIR spectra of neat PCL, porous PCL scaffold prepared at a foaming temperature of 70 °C and TG are reported in Figs. 4a, b and c, respectively. The FTIR spectrum of porous PCL scaffold was nearly the same of that of neat PCL, indicating that any significant differences

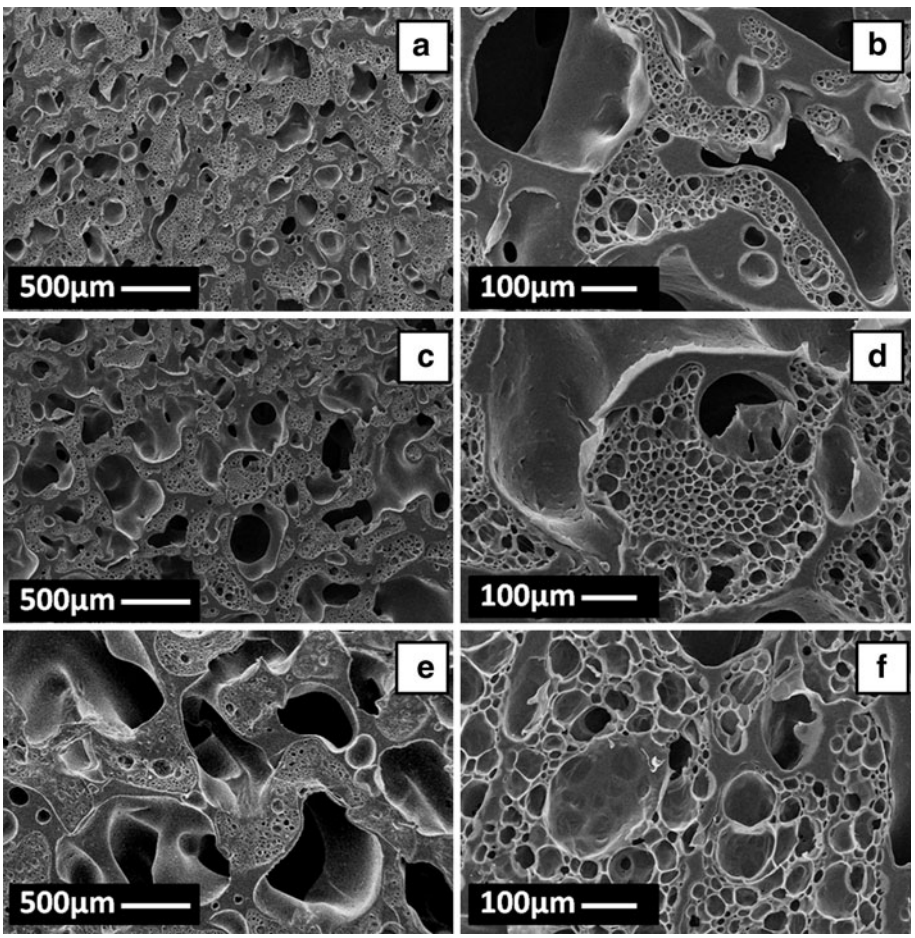

Fig. 1 SEM micrographs of cross-sections of PCL/TG foams prepared at different foaming temperatures: **a**, **b** 70 °C; **c**, **d** 95 °C and **e**, **f** 110 °C

were induced in the chemical structure of the PCL after the gas foaming and TG extraction combined process. In particular, both spectra were characterized by the typical CH_2 stretching in the 2800–3000 cm^{-1}, carbonyl stretching in the 1780–1660 cm^{-1} range and C–O and C–C stretching in the 1290–1300 cm^{-1} range [20, 21]. The absence of the characteristic TG peaks, such as the amide I band at 1650 cm^{-1} (C = O bond stretching and N–H bond bending) and the amide II band at 1540 cm^{-1} (C–N bond stretching, black arrows in Fig. 4c), supported the selective TG extraction results of Fig. 3, indicating the efficiency of the TG extraction process from the scaffolds.

The morphology of the PCL scaffolds resulting from the TG extraction from the foams is reported in Fig. 5, clearly indicating differences with respect to the morphology of the foamed blends (Fig. 1). As expected, after leaching the TG porous network disappeared, resulting in the formation of large pores within the samples. As also observed before the TG extraction, the overall porosity of the PCL scaffolds increased with the increase of the foaming temperature. Nevertheless, all the scaffolds were characterized by elongated pores, probably replicating the initial co-continuous blend morphology [22].

Figure 6 showed the overall porosity of PCL scaffolds as a function of the foaming temperature. In agreement with the morphological results reported in Fig. 5, we observed the increase of the overall porosity with the increase of the foaming temperature. In particular, the overall porosity increased from 60.2 ± 2.5 to 90.3 ± 0.6% when the foaming temperature increased from 70 to 110 °C. It is important to point that, the overall porosity degrees achieved for PCL scaffolds by this approach well

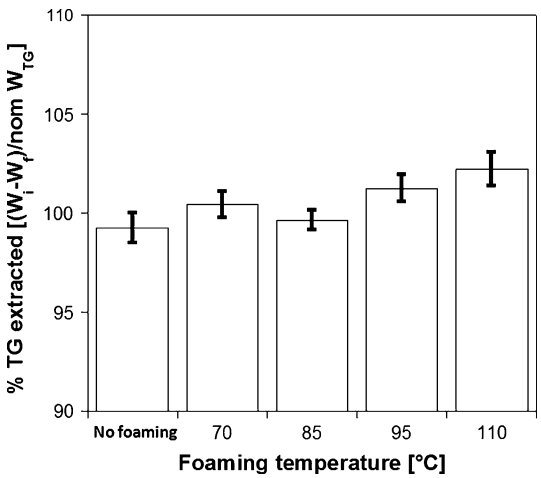

Fig. 3 Percentage of TG extracted from the PCL/TG foams prepared at different foaming temperatures. Neat PCL/TG blend was reported for comparison. W_i and W_f are the weight of the samples before and after leaching; nom W_{TG} is the nominal TG amount

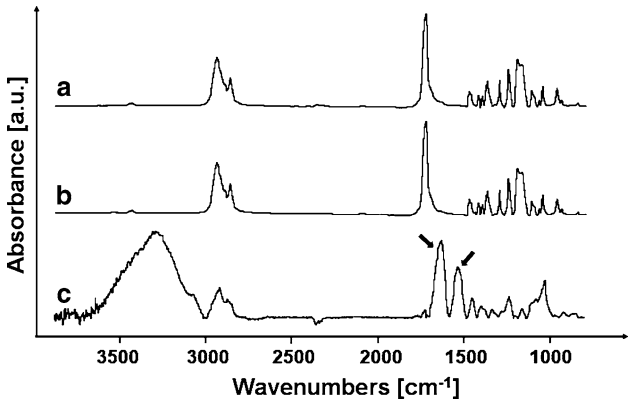

Fig. 4 FTIR spectra of (*a*) neat PCL, (*b*) porous PCL scaffold prepared at a foaming temperature equal to 70 °C and (*c*) TG

match the requirements indicated for TE scaffold applications. For instance, Yilgor et al. and Park et al. prepared PCL scaffolds with overall porosity in the 60 to 90% range by fused deposition modeling and successfully used the as prepared scaffolds for cartilage and bone regeneration applications [23, 24]. Huang et al. also combined PCL scaffolds having porosity of 60% with TGF-b1-loaded fibrin glue to prepare a bioactive scaffold for the in vivo MSCs recruitment [25]. Taking into account these results, the tight control over the overall porosity of PCL scaffolds achievable by the proposed technique, represent a great advantage for TE applications.

Figure 7 reports the effect of the foaming temperature on the mean pore size and pore size distribution of PCL scaffolds. In agreement with the morphological results of Fig. 5, we observed the increase of the mean pore size from 264 ± 119 to 1830 ± 820 μm with the increase of the foaming temperature from 70 to 110 °C (Fig. 7a). Differences were also observed for the pore size distributions of the scaffolds, as shown in Fig. 7b. In particular, the pore size distribution shifted to higher values as the foaming temperature increased and, for the scaffold prepared at 110 °C, we observed a very wide pore size distribution, characterized by pores in the 800–3800 μm range. The increase of pore size with the increase of the foaming temperature has been widely reported in literature for both neat polymers and heterogeneous blends [16, 19, 26]. Indeed, the foaming temperature has a great impact on the rheological properties of polymer/gas solution as well as on the solubility and diffusivity of the blowing agent absorbed within the polymeric matrix, these parameters governing the nucleation and growth of gas bubbles during foaming [16, 19, 26]. In particular, higher foaming temperatures resulted in higher blowing agent diffusivity and lower polymer viscosity, therefore enhancing the growth of gas bubbles within the polymer.

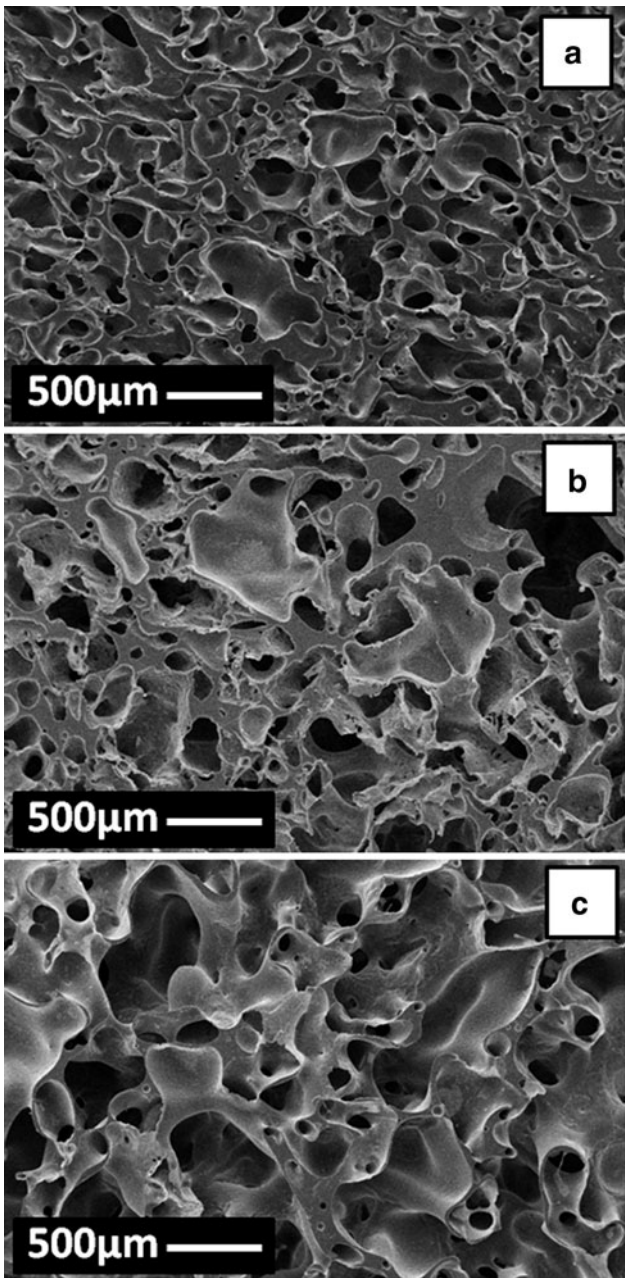

Fig. 5 SEM micrographs of PCL scaffolds prepared after TG extraction from PCL/TG blends foamed at different temperatures: **a** 70 °C; **b** 95 °C and **c** 110 °C

The possibility of controlling the pore size distribution of porous PCL scaffolds by the appropriate selection of the process conditions is a very important design aspect of this technique. There are several studies that indicated the optimal pore size for the specific tissue that it would be regenerated in vitro and in vivo [4, 7, 9]. For instance, Oh et al. recently reported that PCL scaffolds with 380–405 µm pore size are optimal for chondrocytes and osteoblasts growth, while a scaffold pore size in the 186–200 µm range is indicated for fibroblasts growth [13].

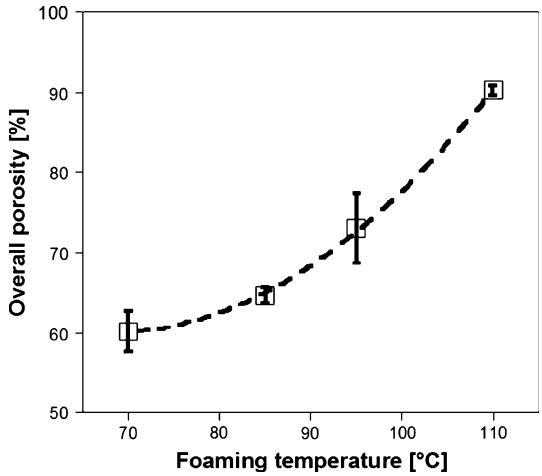

Fig. 6 Effect of foaming temperature on the overall porosity of PCL scaffolds prepared after the selective TG extraction from foamed PCL/TG blend

Furthermore, Woodfield et al. prepared (PEGT/PBT) scaffolds with pore size in the 250–1800 µm range for cartilage regeneration [27]. It is important to point out that, especially at higher foaming temperatures, the mean pore size of the PCL scaffolds are significantly higher than those observed for the PCL phase of the PCL/TG foams (Fig. 2). This effect may be explained by considering that the architecture of the pore structure of PCL scaffolds depends on the foaming of both PCL and TG. As shown in Fig. 2, the foaming of the TG phase increased with the foaming temperature. As a direct consequence, after leaching, the size of the pores created by the selective TG extraction from the PCL/TG foams increased and, the mean pore size and pore size distribution of the scaffolds shifted to higher values (Fig. 7b).

The results of the mechanical characterization performed on the PCL scaffolds are reported in Fig. 8. As shown in Fig. 8a, all the scaffolds were characterized by the typical stress versus strain curve of porous materials undergoing static compression test. In particular, we observed a first linear region, at low strain, related to the elastic behavior, followed by a plateau due to the instability of pore walls and the collapse of the pores and, finally, the steep increase of the stress values at high strains ($\varepsilon > 0.2$ mm/mm) [28, 29]. As expected, the stress versus strain curves shifted to lower stress values as the overall porosity of the PCL scaffolds increased [28, 29]. Accordingly, the elastic modulus decreased from 9.4 ± 1.9 MPa to 1.4 ± 0.5 MPa when the foaming temperature increased from 70 to 110 °C. Similar results were reported by Lebourg et al. and Yao et al. for porous PCL scaffolds prepared by using compression-molding and particle leaching processes [30, 31], indicating that the overall porosity of the scaffolds play a crucial role in defining

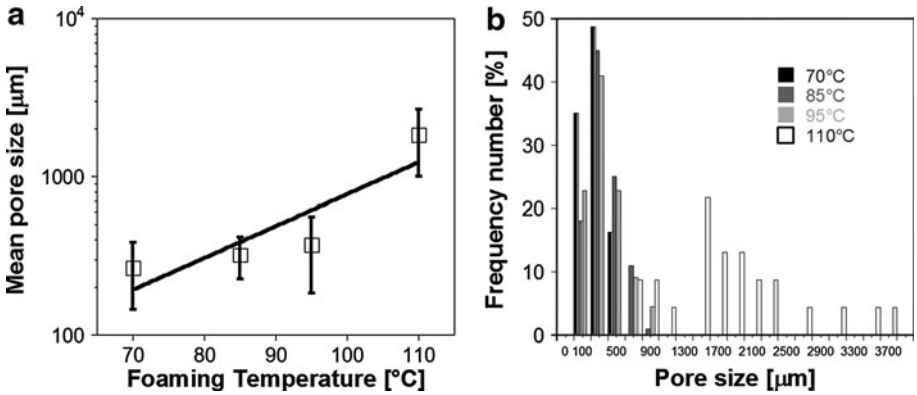

Fig. 7 **a** Mean pore size and **b** pore size distribution of PCL scaffolds as a function of the foaming temperature

theirs mechanical response. Nevertheless, the results of the mechanical characterization indicated that the PCL scaffolds prepared in this study may be used for both soft and hard tissue repair/regeneration [21].

The biocompatibility of PCL scaffolds was assessed in vitro by using hMSCs. Indeed, hMSCs are widely used in tissue engineering and regenerative therapies for their ability to differentiate into a variety of connective tissue lineages, such as bone and cartilage, as well as for their potential to produce new tissues when cultured within tissue-specific scaffolds in vitro and/or in vivo [7, 25, 32]. Taking into account the large number of papers dealing with the bone regeneration properties of hMSCs when cultured within PCL scaffolds, the biocompatibility tests were performed by using the scaffolds prepared at a foaming temperature of 70 °C. Indeed, these scaffolds have micro-structural properties, mainly overall porosity and elastic compression modulus well matching the optimal requirements for bone regeneration applications [21]. The results of these tests are reported in Fig. 9. Differently from the neat scaffold (Fig. 9a), the cross-sections images of the cell/scaffold construct evidenced the MSCs adhesion and infiltration (Figs. 9b, c). In particular, the cells adhered and colonized the porosity close to the seeding surface and, also the interior of the pore structure. The results reported in this study are in agreement with those reported in literature, demonstrating the ability of PCL scaffolds to promote the adhesion and three dimensional colonization of cells in vitro [10, 13, 23, 25, 31].

All these results indicated that the proposed approach allowed the fabrication of porous PCL scaffolds with micro-structural properties and biocompatibility suitable for TE applications.

4 Conclusions

In this study we investigated the design of PCL scaffolds with well controlled pore structures for TE. The scaffolds were prepared by combining GF and reverse templating techniques, this last process based on the selective extraction of the TG from co-continuous PCL/TG blend foams.

The control of PCL scaffold morphology, overall porosity and pore size distributions as well as mechanical properties was achieved by the appropriate selection of foaming temperatures in the 70–110 °C range. In particular, lower foaming temperatures, in the 70–95 °C range, resulted in lower overall porosity and pore size and higher scaffold mechanical properties. Conversely, PCL scaffolds

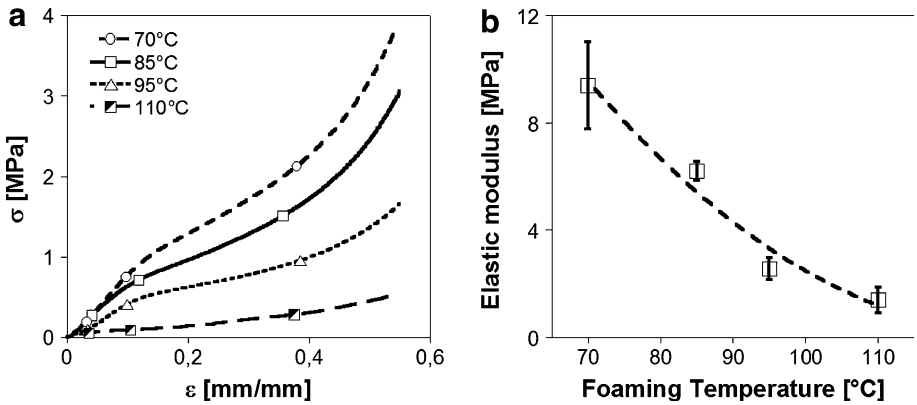

Fig. 8 **a** Representative tress versus strain curves and **b** elastic compression modulus resulting from the compression tests performed on PCL scaffolds

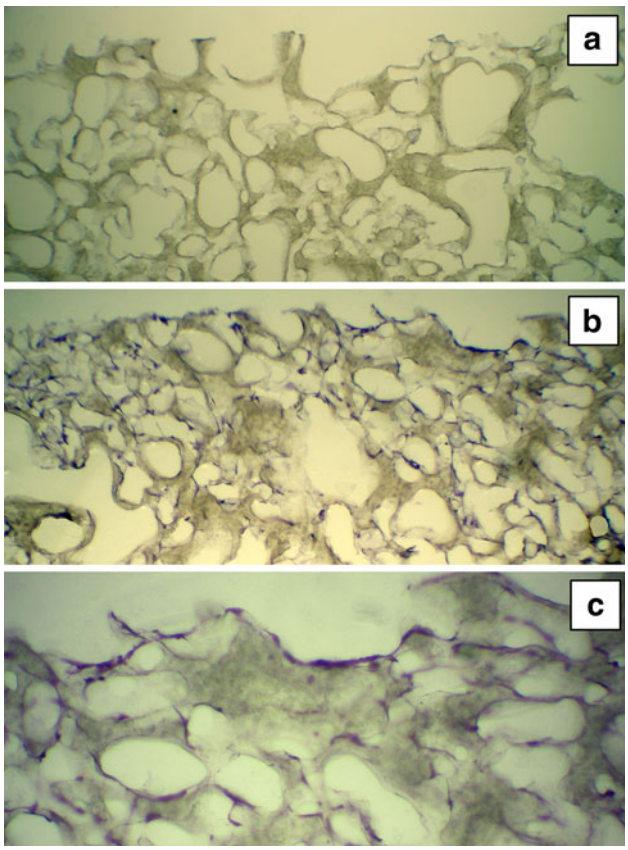

Fig. 9 H&E staining of the cross-sections of **a** PCL and **b**, **c** MSCs/PCL scaffold construct after 1 week of in vitro culture. The reported scaffold was prepared at a foaming temperature of 70 °C

with high degree of overall porosity (up to 90%) and large pore size, in the 800–3800 μm range, were prepared at a foaming temperature of 110 °C.

The obtained scaffolds were also capable to allow for the in vitro adhesion and colonization of MSCs.

We may therefore conclude that the GF and selective TG extraction combined approach may be efficiently used to design PCL scaffolds for TE applications.

Acknowledgments The authors thank Daniela Guarnieri, Maria Iannone and Stefania Zeppetelli for theirs contribute to the biological characterization of the scaffolds.

References

1. F. Causa, P.A. Netti, L. Ambrosio, Biomaterials **28**, 5093 (2007)
2. V. Liu.Tsang, S.N. Bhatia, Adv. Drug Deliv. Rev. **56**, 1635 (2004)
3. E. Chevalier, D. Chulia, C. Pouget, M. Viana, J. Pharm. Sci. **97**, 1135 (2008)
4. S. Yang, K. Leong, Z. Du, C. Chua, Tissue Eng. **7**, 679 (2001)
5. S.J. Hollister, Nat. Mater. **4**, 518 (2005)
6. H. Sung, C. Meredith, C. Johnson, Z.S. Galis, Biomaterials **25**, 5735 (2004)
7. V. Karageorgiou, D. Kaplan, Biomaterials **26**, 5474 (2005)
8. T.G. van Tienen, R.G.J.C. Heijkants, P. Buma, J.H. de Groot, A.J. Pennings, R.P.H. Veth, Biomaterials **23**, 1731 (2002)
9. E. Pamula, L. Bacakova, E. Filova, J. Buczynska, P. Dobrzynski, L. Noskova, L. Grausova, J. Mater. Sci. Mater. Med. **19**, 425 (2008)
10. A. Salerno, D. Guarnieri, M. Iannone, S. Zeppetelli, E. Di Maio, S. Iannace, P.A. Netti, Acta Biomater. **5**, 1082 (2009)
11. L.E. Freed, G. Vunjak-Novakovic, R.J. Biron, D.B. Eagles, D.C. Lesnoy, S.K. Barlow, R. Langer, Nat. Biotech. **12**, 689 (1994)
12. A.J. Marshall, A.C. Irvin, T. Barker, H.E. Sage, K.D. Hauch, B.D. Ratner, Polym. Prepr. **45**, 100 (2004)
13. S.H. Oh, I.K. Park, J.M. Kim, J.H. Lee, Biomaterials **28**, 1664 (2007)
14. C.E. Petrie Aronin, K.W. Sadik, A.L. Lay, D.B. Rion, S.S. Tholpady, R.C. Ogle, E.A. Botchwey, J. Biomed. Mater. Res. Part A, 89, 632 (2009)
15. M.H. Sheridan, L.D. Shea, M.C. Peters, D.J. Mooney, J. Contr. Rel. **64**, 91 (2000)
16. H. Tai, M.L. Mather, D. Howard, W. Wang, L.J. White, J.A. Crowe, S.P. Morgan, A. Chandra, D.J. Williams, S.M. Howdle, K.M. Shakesheff, Eur. Cells Mater. **14**, 64 (2007)
17. A. Léonard, C. Calberg, G. Kerckhofs, M. Wevers, R. Jérôme, J. Pirard, A. Germain, S. Blacher, J. Porous. Mater. **15**, 397 (2008)
18. L.D. Harris, B. Kim, D.J. Mooney, J. Biomed. Mater. Res. **42**, 396 (1998)
19. A. Salerno, M. Oliviero, E. Di Maio, S. Iannace, Int. Polym. Proc. **5**, 480 (2007)
20. D. Pankajakshan, L.P. Philipose, M. Palakkal, K. Krishnan, L.K. Krishnan, J. Biomed. Mater. Res. Part B: Appl. Biomater. 87B, 570 (2008)
21. L. Ghasemi-Mobarakeh, M.P. Prabhakaran, M. Morshed, M. Nasr-Esfahani, S. Ramakrishn, Biomaterials **29**, 4532 (2008)
22. A. Salerno, M. Oliviero, E. Di Maio, S. Iannace, P.A. Netti, J. Mater. Sci. Mater. Med. **20**, 2043 (2009)
23. P. Yilgor, R.A. Sousa, R.L. Reis, N. Hasirci, V. Hasirci, Macromol. Symp. **269**, 92 (2008)
24. S. Park, G. Kim, Y.G. Jeon, Y. Koh, W. Kim, J. Mater. Sci. Mater. Med. **0**, 229 (2009)
25. Q. Huang, J.C.H. Goh, D.W. Hutmacher, E.H. Lee, Tissue Eng. **8**, 469 (2002)
26. W. Zhai, H. Wang, J. Yu, J. Dong, J. He, J. Polym. Sci. Part B Polym. Phys. **46**, 1641 (2008)
27. T.B.F. Woodfield, J. Malda, J. de Wijn, F. Péters, J. Riesle, C.A. van Blitterswijk, Biomaterials **25**, 4149 (2004)
28. A. Salerno, E. Di Maio, S. Iannace, P.A. Netti, J. Cell. Plast. **45**, 109 (2009)
29. Q. Liu, G. Subhash, X. Gao, J. Porous. Mater. **12**, 233 (2005)
30. M. Lebourg, R.S. Serra, J.M. Estellés, F.H. Sánchez, J.L.G. Ribelles, J.S. Antón, J. Mater. Sci. Mater. Med. **19**, 2047 (2008)
31. D. Yao, A. Smith, P. Nagarajan, A. Vasquez, L. Dang, G.R. Chaudhry, J. Biomed. Mater. Res. Part B Appl. Biomater. **77B**, 287 (2006)
32. A. Salerno, D. Guarnieri, M. Iannone, S. Zeppetelli, P.A. Netti, Tissue Eng. **16**, 2661 (2010)